Biochimica et Biophysica Acta 1809 (2011) 211–219

Contents lists available at ScienceDirect

Biochimica et Biophysica Acta

journal homepage: www.elsevier.com/locate/bbagrm

Biochemical characterization of enterovirus 71 3D RNA polymerase

Hongbing Jiang [a], Leiyun Weng [a], Na Zhang [a], Minetaro Arita [b], Renqing Li [c], Lijuan Chen [c], Tetsuya Toyoda [a,d,e,*]

[a] Unit of Viral Genome Regulation, Institut Pasteur of Shanghai, Key Laboratory of Molecular Virology & Immunology, Chinese Academy of Sciences, Shanghai, PR China
[b] Department of Virology II, National Institute of Health, Tokyo, Japan
[c] Beijing Center for Disease Control and Prevention, Beijing, PR China
[d] Choju Medical Institute, Fukushimura Hospital, 19-4 Azanakayama, Noyori-cho, Toyohashi, Aichi 441-8124, Japan
[e] Infectious Disease Regulation Project, Tokyo Metropolitan Institute of Medical Sciences, 1-6, Kamikitazawa 2-chome, Setagaya-ku, Tokyo156-8506, Japan

ARTICLE INFO

Article history:
Received 4 October 2010
Received in revised form 27 December 2010
Accepted 3 January 2011
Available online 8 January 2011

Keywords:
Enterovirus 71
3D protein
RNA polymerase
Transcription
Km
Vmax

ABSTRACT

An unusual enterovirus 71 (EV71) epidemic has begun in China since 2008. EV71 RNA polymerases ($3D^{pol}$) showed polymerase activity with an Mn^{2+}. Little activity was detected with Co^{2+}, and no activity was detected with Mg^{2+}, Ca^{2+}, Cu^{2+}, Ni^{2+}, Cd^{2+}, or Zn^{2+}. It is a primer-dependent polymerase, and the enzyme functioned with both di- and 10-nucleotide RNA primers. DNA primer, dT15, increased primer activity, similar to other enterovirus $3D^{pol}$. However, EV71 $3D^{pol}$ initiated *de novo* transcription with a poly(C) template and genome RNA. Its RNA binding activity was weak. Terminal nucleotidyl transferase and reverse transcriptase activity were not detected. The *K*m and *V*max for EV71 $3D^{pol}$ were calculated from classic Lineweaver–Burk plots. The *K*m values were 2.35 ± 0.05 (ATP), 5.40 ± 0.93 (CTP), 1.12 ± 0.10 (GTP) and 2.81 ± 0.31 (UTP), and the *V*max values were 0.00078 ± 0.00005/min (ATP), 0.011 ± 0.0017/min (CTP), 0.050 ± 0.0043/min (GTP) and 0.0027 ± 0.0005/min (UTP). The *K*m of EV71 $3D^{pol}$ was similar to that of foot and mouth disease virus and rhinovirus. Polymerase activity of BrCr-TR strain and a strain from a clinical isolate in Beijing, 2008 were similar, indicating the potential for $3D^{pol}$ as an antiviral drug target.

1. Introduction

Enterovirus 71 (EV71) is a small, non-enveloped virus with a single-stranded, positive-sense RNA genome of about 7500 nucleotides (nt) and belongs to the genus *Enterovirus* of the family *Picornaviridae* [1]. *Picornaviridae* genomes are not capped, but rather they are covalently linked to a 22-amino-acid viral peptide called VPg. The 5′ untranslated region of these genomes contains an internal ribosome entry site (IRES), which is the site of initiation of translation. *Picornaviridae* genomes are polyadenylated at their 3′ ends. One large polyprotein precursor of approximately 250 kDa is encoded by genomes of *Picornaviridae*, which consists of one structural region (P1) and two nonstructural regions (P2 and P3) in a single open reading frame. This large polyprotein precursor is processed via autoproteolysis by viral proteases $2A^{pro}$, $3C^{pro}$, and $3CD^{pro}$, resulting in a variety of precursor and mature viral proteins. P3 is processed into the 3AB and $3CD^{pro}$ proteins. 3AB is further processed into the membrane-anchor protein 3A and the protein 3B, also called VPg. $3CD^{pro}$ is further processed into the proteins $3C^{pro}$ and $3D^{pol}$, which is the viral RNA-dependent RNA polymerase (RdRp).

Picornaviridae RdRps use the viral protein VPg as a primer for positive-strand and negative-strand viral RNA synthesis. VPg is uridylated by $3D^{pol}$, which covalently links two UMP molecules to the third amino acid residue of VPg, a tyrosine (Y3). For enteroviruses, this reaction is templated either by a *cis*-acting replication element (*cre*), which is an RNA stem-loop structure situated in the coding region of protein 2C [*cre* (2C)], or by the poly(A) tail, albeit with lower efficiency *in vitro* [2].

EV71 is classified as a *Human enterovirus species A*, along with some coxsackie A viruses (CVA), such as CVA10 and CVA16, which cause hand, foot and mouth disease (HFMD), and herpangina. Phylogenetic analysis of EV71 1D coat protein has demonstrated the three genetic lineages: genotype A, B and C [3], which can be further subdivided into genogroups: B1 to B5 and C1 to C5 [4–7]. EV71 infections are sometimes associated with severe neurological diseases, such as brain stem encephalitis and poliomyelitis-like paralysis, although most EV71 infections commonly result in self-limiting conditions [8]. A number of fatal encephalitis cases were reported during large-scale HFMD

Abbreviations: $3D^{pol}$, 3D polymerase; BJ, Beijing; *cre*, *cis*-acting replication element; CV, coxsackie virus; *E. coli*, *Escherichia coli*; EV71, enterovirus 71; FBS, fetal bovine sera; FMDV, foot-and-mouth disease virus; HCV, hepatitis C virus; HFMD, hand foot mouth disease; HRV, human rhino virus; IRES, internal ribosome entry site; MEM, minimal essential media; MuLV, murine leukemia virus; PAGE, polyacrylamide gel electrophoresis; RD, rhabdomyosarcoma; RTase, reverse transcriptase; RdRp, RNA dependent RNA polymerase; SPR, surface plasmon resonance; Tm, melting temperature; knt, kilonucleotide; nt, nucleotide

* Corresponding author. Choju Medical Institute, Fukushimura Hospital, 19-4 Azanakayama, Noyori-cho, Toyohashi, Aichi 441-8124, Japan. Tel.: +81 532 46 7511; fax: +81 532 46 8940.
E-mail address: toyoda_tetsuya@yahoo.co.jp (T. Toyoda).

1874-9399/$ – see front matter © 2011 Elsevier B.V. All rights reserved.
doi:10.1016/j.bbagrm.2011.01.001

outbreaks in Malaysia in 1997 [9] and in Taiwan in 1998 and 2000 [10,11]. Most of the fatal cases of EV71 during the outbreaks in Taiwan were caused by pulmonary edema and/or pulmonary hemorrhage, which may have been caused by direct destruction of the vasomotor and respiratory centers in the brain stem by EV71 infection [10,12–16]. A presently ongoing EV71 epidemic that began in 2008 in China resulted in 126 fatalities out of 481,000 total EV71 cases in 2008 [17–19]. Pyrimidine derivatives [20], and more recently, DTriP-22 (4{4-[(2-bromo-phenyl)-(3-methyl-thiophen-2-yl)-methyl]-piperazin-1-yl}-1-pheny-1*H*-pyrazolo[3,4-*d*]pyrimidine) were found to target EV71 3Dpol [21]. To date, however, no effective vaccine or antiviral drugs against EV71 have been available yet.

Because RdRps of RNA viruses are essential for viral replication, and an equivalent host cellular enzyme does not exist, these polymerases are prime targets for the development of antiviral drugs. The ternary structure of EV71 3D^{pol} of the Chinese epidemic strain was revealed recently [22]. However, the biochemical feature of the RdRp has not been analyzed enough. In order to study the contribution of RdRp activity to the pathogenicity of EV71, and to develop anti-EV71 3D^{pol} drugs, we analyzed the biochemical characteristics including kinetic data of the EV71 3D^{pol}, which consists of 463 amino acids and which calculated molecular weight is 53 kDa, of the prototype strain, BrCr-TR (group A), and compared our findings to the polymerase activity of an isolate from a severe HFMD case collected in Beijing in 2008 (EV71 BJ), which belongs to group C [23].

2. Materials and methods

2.1. Cell culture

Human rhabdomyosarcoma (RD) cells were maintained in minimal essential media (MEM, GIBCO) supplemented with 10% fetal bovine sera (FBS, GIBCO), 2 mM L-Glutamine (GIBCO), 100 U/ml penicillin G sodium, and 100 μg/ml streptomycin sulfate (GIBCO).

2.2. Isolation and cDNA construction of enterovirus 71

Enterovirus 71 (EV71 BJ) was isolated from a skin vesicle from a severely ill HFMD patient in Beijing, China, in 2008, and cultured in RD cells. Viral RNA was extracted from the culture media using the QIAamp Mini Viral RNA Extraction Kit (Qiagen). cDNA of EV71 BJ (GenBank account No. FJ606449) was amplified by RT-PCR as two fragments from viral RNA using the OneStep RT-PCR kit (Qiagen) and the primers listed in Table S1.

2.3. Construction of plasmids expressing EV71 3D^{pol}

EV71 3D^{pol} was PCR-amplified from pEV71(BrCr-TR) [24] and the PCR fragment of EV71 BJ using BrCr-TR-N and C, and BJ-N and C (Table S1) by Pyrobest (Takara), and A-addition by LA-taq (Takara) before being cloned into the pGEMT vector (Promega). After digestion with NdeI and XhoI, EV71BrCr-TR 3D^{pol} was cloned into the same sites of pET21b(KM) [25], resulting in pETEV71(BrCr-TR)3D^{pol}. The polymerase knock-out mutation, D330A was introduced using an *in vitro* mutagenesis kit (Stratagene, Table S1) to yield the construct pETEV71 (BrCr-TR)3D^{pol}D330A. The PCR fragment of EV71 BJ was cloned into pET21b(KM), resulting in pETEV71(BJ)3D^{pol}. Construct sequences were confirmed by DNA sequencing (Invitrogen).

2.4. Expression and purification of EV71 3D^{pol}

pETEV71(BrCr-TR)3D^{pol}, pETEV71(BrCr-TR)3D^{pol}D330A and pETEV71(BJ)3D^{pol} were transformed into *Escherichia coli* (*E. coli*) Rosetta/pLysS (Novagen). The expression of EV71 3D^{pol} was induced with 1 mM IPTG at 37 °C for 1 h after the bacteria had been grown to AD600 = 0.58. After harvesting, the cells were suspended in a buffer containing 50 mM NaH_2PO_4 (pH 8.0), 500 mM NaCl, 0.1% Triton X-100, 0.1% 2-mercaptoethanol, 1 mM PMSF, and 2 mM imidazole and lysed by sonication. After centrifugation at 11,000 rpm for 30 min at 4 °C (Beckman JA rotor), the supernatant was incubated with Ni-NTA agarose (Qiagen), and the bound EV71 3D^{pol} was eluted with elution buffer (20 mM Tris–HCl (pH 8.0), 500 mM NaCl, 0.1% Triton X-100, and 0.1% 2-mercaptoethanol) containing 250 mM imidazole after the column had been washed with 40 mM imidazole. EV71 3D^{pol} was chromatographed on Superdex200 (GE) in 20 mM Tris–HCl (pH 8.0), 500 mM NaCl, 1 mM EDTA, 1 mM DTT, and 1 mM PMSF, followed by further chromatography on MonoQ (GE) in 20 mM Tris–HCl (pH 8.0), 50 mM NaCl, 1 mM EDTA, 1 mM DTT, and 1 mM PMSF. EV71 3D^{pol} was eluted with 220 mM NaCl. The purified EV71 3D^{pol} was stored at −80 °C.

2.5. EV71 genome RNA

EV71 BrCr-TR strain genome RNA was transcribed *in vitro* from MluI-linearized pEV71 (BrCr-TR) [24] using the MegaScript T7 kit (Ambion) (Fig. S1).

2.6. In vitro transcription

One hundred nanomolars of EV71 3D^{pol} were incubated in 50 mM Tris–HCl (pH 7.5), 7 mM $MnCl_2$, 100 mM potassium-monoglutamate, 1 mM DTT, 25 μg/ml actinomycin D, 0.05 mM [α-^{32}P] UTP, 1 μM U10, 200 U/ml RNase inhibitor, and 2 mg/ml poly(A) at the indicated temperature (29 °C) and for the indicated time (90 min). After phenol-chloroform extraction and ethanol precipitation, the transcripts were analyzed by 4% PAGE containing 8 M urea, followed by image analysis with Typhoon Trio plus (GE). For pH sensitivity analysis, 50 mM of HCl–KCl (pH 2), glycine-HCl (pH 3), MES-NaOH (pH 4.0 and 5.0), MOPS-NaOH (pH 6.0 and 6.5), 50 mM Tris–HCl (pH 7.0, 7.5, 8.0, 8.5, and 9.0), and CAPS-NaOH (pH 10) were used. For kinetic analysis, [α-^{32}P] ATP, poly(U), and A10 were used for ATP; [α-^{32}P] GTP, poly(C), and G10 were used for GTP; and [α-^{32}P] CTP, poly(I), and C10 were used for CTP. After phenol/chloroform extraction and ethanol precipitation, RNA transcripts were separated by 4% polyacrylamide gel electrophoresis (PAGE) containing 8 M urea in 0.5 × TBE (44.5 mM Tris–HCl, 44.5 mM borate, 1 mM EDTA).

In vitro transcription was also performed using the sym/sub template [26]. 5′-[^{32}P]-sym/sub (1 μM) was mixed with non-labeled sym/sub (99 μM) and annealed in TE by gradual cooling down for 5 °C/min from 90 °C to 10 °C after denaturation at 90 °C for 1 min. The annealed sym/sub (2 and 10 pmol) were incubated with 100 nM EV71 3D^{pol} in 50 mM Tris–HCl (pH 7.5), 7 mM $MnCl_2$, 100 mM potassium-monoglutamate, 1 mM DTT, 25 μg/ml actinomycin D, 0.5 mM ATP, CTP, GTP, and UTP, 200 U/ml RNase inhibitor. After phenol/chloroform extraction and ethanol precipitation, the syn/sub transcripts were separated by 15% PAGE containing 6 M urea in 0.5 × TBE.

The incorporated radioisotopes were measured by Typhoon Trio plus. The mean and standard deviations of the incorporated amounts of NMP were calculated from three independent experiments.

2.7. Reverse transcriptase assay

One hundred nanomolars of EV71 3D^{pol} were incubated in 50 mM Tris–HCl (pH 7.5), 7 mM $MnCl_2$, 100 mM potassium-monoglutamate, 1 mM DTT, 25 μg/ml actinomycin D, 0.05 mM [α-^{32}P] TTP, 1 μg/ml dT15, 200 U/ml RNase inhibitor, and 20 μg/ml A32. As a control, A32 was reverse transcribed from murine leukemia virus reverse transcriptase (MuLV RTase) according to the company's instruction. After phenol/chloroform extraction and ethanol precipitation, the products were separated by 12% PAGE containing 6 M urea in 0.5 × TBE.

2.8. RNA filter binding assay

The filter binding assay of EV71 $3D^{pol}$ and [^{32}P]-EV71 BrCr-TR genome RNA was performed as previously published [27]. Hepatitis virus (HCV) JFH1 NS5B RNA polymerase was used as a control [27]. Briefly, [^{32}P]-EV71 BrCr-TR genome RNA was transcribed *in vitro* by T7 RNA polymerase (Takara) with [α-^{32}P]UTP (New England Nuclear). After incubation, un-incorporated [α-^{32}P]UTP was removed by gel filtration in a Quick Spin G-50 (Roche), and [^{32}P]-EV71 BrCr-TR genome RNA was purified by phenol/chloroform extraction and ethanol precipitation. The filter binding assay was conducted using the method of Oberste and Flanegan [28]. Five picomols of the RdRp and 5 pmol of [^{32}P]-EV71 BrCr-TR genome RNA were incubated at 30 °C for 30 min in 25 μl of 50 mM Tris–HCl (pH 7.5), 7 mM $MnCl_2$, 100 mM potassium-monoglutamate and 1 mM DTT. After incubation, the solutions were diluted with 0.5 ml TE and filtered through nitrocellulose membranes (0.45 μm, Millipore), which were boiled in TE for 30 min before the experiment. The filter was washed 5 times with TE and the bound radioisotope was analyzed by Typhoon Trio plus after being dried.

2.9. RNA crosslink assay

v84 influenza virus model RNA templates [29] was transcribed *in vitro* by T7 RNA polymerase with [α-^{32}P]UTP. One picomol of RdRp in the presence of 1 pmol [^{32}P]-labeled v84 or EV71 BrCr-TR genome RNA in a 10 μl reaction containing 50 mM Tris–HCl (pH 7.5), 7 mM $MnCl_2$, 100 mM potassium-monoglutamate and 1 mM DTT was incubated at 30 °C for 30 min. Reactions were then UV irradiated (254 nm) for 30 min on ice, and the cross-linked products were separated by 10% SDS-PAGE after RNase A (0.1 mg/ml) treatment. Cross-linked proteins were analyzed by Typhoon Trio plus.

2.10. Surface plasmon resonance (SPR) biosensor analysis

Twenty micrograms per mililiter of EV71 $3D^{pol}$, hepatitis C virus (HCV) JFH1 NS5B RdRp [27] and bovine serum albumin (BSA) were immobilized by amine coupling to the parallel channel of CM5 biosensor chip (GE) in phosphate buffered saline (PBS, pH 7.2), resulting in surface densities of 2000 to 5000 response units. SPR measurements were performed with the BIAcore T100 instrument (GE) equilibrated at 25 °C. Poly(A), poly(U), poly(G), poly(I) and poly(C) at 0.2 mg/ml PBS were injected for 3 min across the immobilized proteins at a flow rate of 20 μl/min. Following each injection, the biosensor chip was regenerated with 5 mM NaOH. Interactions of RNA templates with both HCV NS5B and EV71 3D polymerases were monitored in real time and reflected by response units, which were calculated by subtraction of the BSA reference channel.

2.11. Chemicals and radioisotopes

Actinomycin D, MES, MOPS, Tris (Trizma), BSA, poly(A), poly(U), poly(G), poly(I), poly(C), and UpU were obtained from Sigma; nucleotides were purchased from GE; [α-^{32}P] UTP, [α-^{32}P] ATP, [α-^{32}P] GTP, [α-^{32}P] CTP, [α-^{32}P] TTP and [γ-^{32}P]ATP were purchased from New England Nuclear; dinucleotide primers (ApA, GpG and CpC), oligonucleotide primers (A10, A32, U10, U16, G10, G18, C10, C27, dT10 and dT15), human placental RNase inhibitor, T4 nucleotide kinase, MuLV RTase and restriction enzymes were purchased from Takara; and other oligonucleotides were from Invitrogen.

2.12. Statistical analysis

Statistical data were evaluated by the Student's *t* test.

3. Results

3.1. Purification of EV71 $3D^{pol}$

C-terminal 6xHis-tagged EV71 3D polymerase ($3D^{pol}$) of BrCr-TR strain (BrCr-TR), its polymerase knock-out mutant (D330A) and a Beijing isolate (BJ) were expressed in bacteria and purified by Ni-NTA column chromatography, followed by gel-filtration through Superdex200 in 20 mM Tris–HCl (pH 8.0), 0.5 M NaCl, 1 mM DTT, and 1 mM EDTA. Finally, the 44 kDa elution fraction was applied to MonoQ anion exchange chromatography and eluted at 220 mM NaCl (Figs. 1 and 2A).

3.2. Biochemical analysis of EV71 $3D^{pol}$

The purified EV71 $3D^{pol}$ was gel-filtrated at approximately 44 kDa from the Superdex200 column in 20 mM Tris–HCl (pH 7.5), 100 mM NaCl, 1 mM DTT, and 1 mM EDTA, which indicated that the EV71 $3D^{pol}$ formed a monomer under these transcription conditions *in vitro* (Fig. 2B).

The biochemical characteristics of EV71 BrCr-TR $3D^{pol}$ are presented in Figs. 3 and 4. Optimal *in vitro* primer-dependent transcription activity of EV71 BrCr-TR $3D^{pol}$ was observed with 50 mM Tris–HCl (pH 7.5), 100 mM potassium-monoglutamate, 7 mM $MnCl_2$, 1 mM DTT, 50 μM [α-^{32}P]UTP, 2 mg/ml poly(A) RNA template, 0.5 μM U10 primer (or 0.5 mM UpU), 25 μg/ml actinomycin D, 200 U/ml human placental RNase inhibitor, and 100 nM EV71 $3D^{pol}$ at 29 °C for 90 min. The EV71 BrCr-TR $3D^{pol}$ D330A abolished polymerase activity (Fig. 3A), indicating that amino acid residues GDD (at positions 329–331) comprise the polymerase active site.

First, the requirement of either $MgCl_2$ or $MnCl_2$ on polymerase activity was tested at 0, 1, 2, 3, 4, 4.5, 5, 6, 7, 8, 9, 10, 11, 13, 15, and 20 mM $MgCl_2$ or $MnCl_2$ in 50 mM Tris–HCl (pH 7.5), 100 mM NaCl, 1 mM DTT, 25 μg/ml actinomycin D, 50 μM [α-^{32}P] UTP, 200 U/ml RNase inhibitor, 100 nM $3D^{pol}$, 2 mg/ml poly(A) RNA, and 0.5 mM UpU (Fig. 4A). Polymerase activity of EV71 BrCr-TR $3D^{pol}$ gradually increased starting at 1 mM $MnCl_2$, and the maximal activity (0.154 ± 0.004 pmol UMP/pmol $3D^{pol}$; polymerase activity is expressed per 1 pmol $3D^{pol}$ in the text) was seen at 4.5 mM $MnCl_2$. The polymerase activity decreased quickly above concentrations of 5 mM $MnCl_2$. EV71 BrCr-TR $3D^{pol}$ did not show polymerase activity with $MgCl_2$. Next, $MnCl_2$ and $MgCl_2$ sensitivity were tested in 100 mM potassium-monoglutamate buffer, in which the polymerase activity was 100 times higher than that with NaCl (Fig. 4B). In 100 mM potassium-monoglutamate buffer, the highest polymerase activity (14.8 ± 1.6 pmol UMP) was observed at 7 mM $MnCl_2$. The $MnCl_2$ dependency curves in NaCl and potassium-monoglutamate were different. In potassium-monoglutamate buffer, the $MnCl_2$ dependency curve stretched from 1 to 15 mM in a symmetrical shape, with 7 mM as the peak activity. EV71 $3D^{pol}$ did not show any polymerase activity with $MgCl_2$ and no polymerase activity with the dT15 primer was detected under the same conditions (Fig. 4B). Other divalent cations such as $CoCl_2$, $CaCl_2$, $CuCl_2$, $NiCl_2$, $CdCl_2$, and $ZnCl_2$ were each tested at 7 mM in 100 mM potassium-monoglutamate buffer (Fig. 4C). EV71 $3D^{pol}$ displayed low polymerase activity (0.094 ± 0.005 pmol UMP) with $CoCl_2$. EV71 $3D^{pol}$ did not display any polymerase activity with the other divalent cations.

The dependency of polymerase activity on monovalent cations such as NaCl, KCl, sodium, and potassium-monoglutamate was tested at 0, 50, 100, 150, 200, 250, 300, 400, and 1000 mM with 7 mM $MnCl_2$ (Fig. 4D). EV71 $3D^{pol}$ showed higher polymerase activity with K^+ rather than Na^+. The highest polymerase activity (10.7 ± 0.8 pmol UMP) was obtained at 100 mM potassium-monoglutamate. In KCl the highest polymerase activity (4.83 ± 1.0 pmol UMP) was observed at 50 mM. With NaCl, EV71 $3D^{pol}$ displayed low polymerase activity (0.619 ± 0.058 pmol UMP), with maximal activity observed at

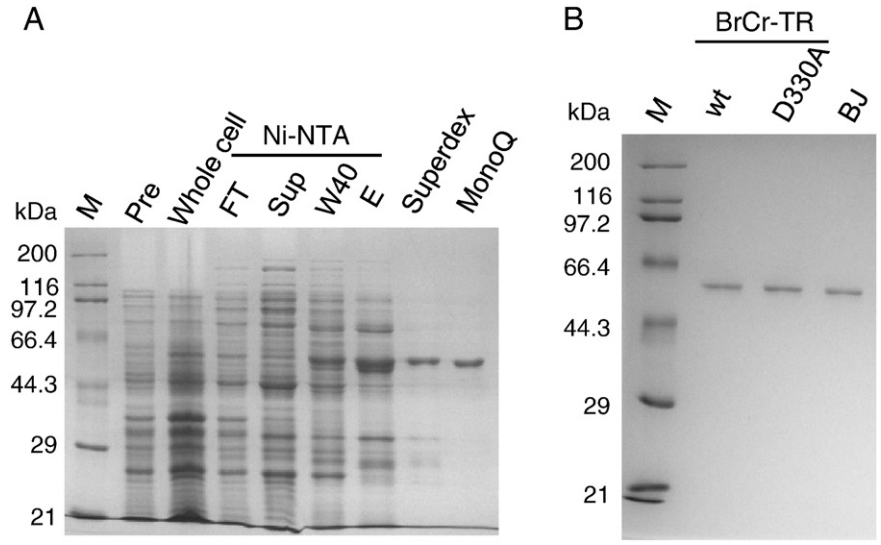

Fig. 1. Purification of EV71 3D^{pol}. A: SDS-PAGE for the purification of EV71 BrCr-TR 3D^{pol}. Ten microliters of each fraction were run on 10% SDS-PAGE and stained with Coomassie brilliant blue. M: standard size marker (Takara). Pre: pre-induced bacterial lysate. Sup: soluble fraction of the bacterial extract after IPTG induction. FT: flow through fraction of Ni-NTA. W40: fraction washed from Ni-NTA with 40 mM imidazole. E: fraction eluted from Ni-NTA with 250 mM imidazole. Superdex: elution fraction of Superdex200 after Ni-NTA column chromatography. MonoQ: elution fraction of MonoQ. B: SDS-PAGE of the purified EV71 BrCr-TR 3D^{pol} wild type (wt), the polymerase knock-out mutant (D330A) and Beijing isolate (BJ). M: standard size marker. The position of the molecular standard marker (kDa) is indicated on the left.

150 mM. For sodium-monoglutamate, the highest activity (4.13 ± 0.51 pmol UMP) was obtained at 100 mM, but decreased to 0.9 ± 0.21 pmol UMP at 50 mM. At high salt concentrations (more than 400 mM for sodium and potassium-monoglutamate and NaCl and more than 150 mM for KCl), EV71 3D^{pol} did not show polymerase activity.

Dependency of polymerase activity on pH was tested from pH 2 to 10 with 4.5 mM $MnCl_2$ and 100 mM potassium-monoglutamate

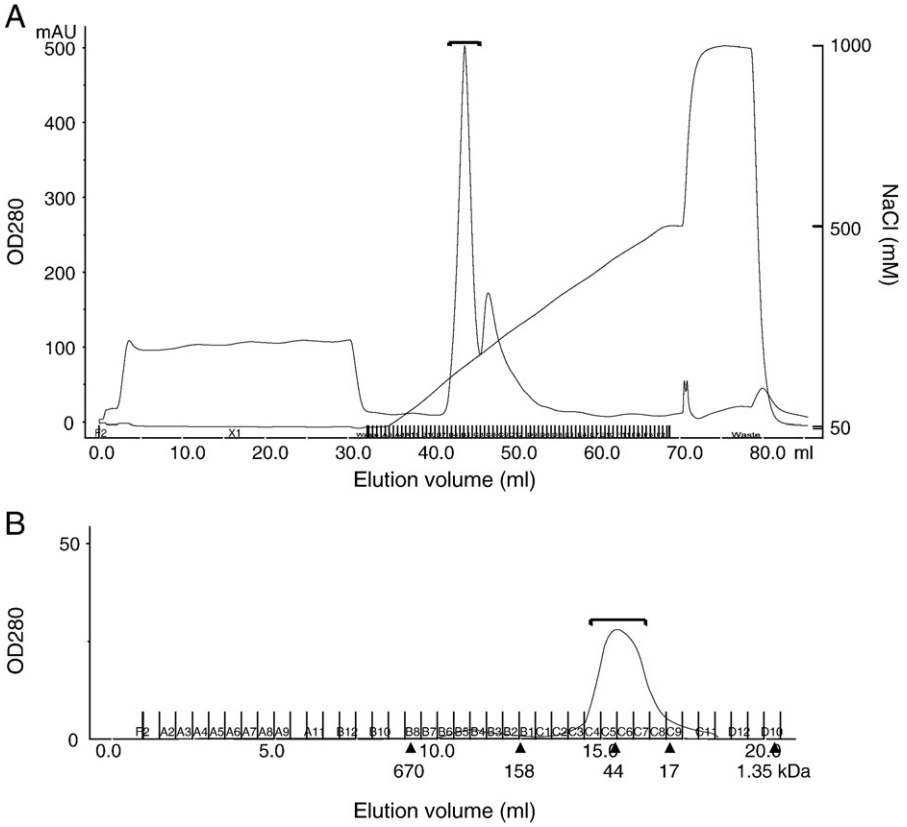

Fig. 2. Column chromatography of EV71 3D^{pol}. A: MonoQ anion exchange column chromatography of EV71 3D^{pol}. EV71 3D^{pol} expressed in bacteria was finally purified by MonoQ anion exchange chromatography using a continuous NaCl gradient from 50 to 1000 mM, after purification on Ni-NTA column chromatography and gel-filtration by Superdex200. EV71 3D^{pol} was eluted with 220 mM NaCl as indicated on the graph. B: gel-filtration of EV71 3D^{pol}. The purified EV71 BrCr-TR 3D^{pol} was applied to Superdex200 in the standard transcription buffer (20 mM Tris–HCl (pH 7.5), 100 mM potassium-monoglutamate, 1 mM DTT, and 1 mM EDTA). The migration position of EV71 3D^{pol} is indicated in the figure. The migration positions of Gel Filtration Standard (BioRad) are indicated below the graph.

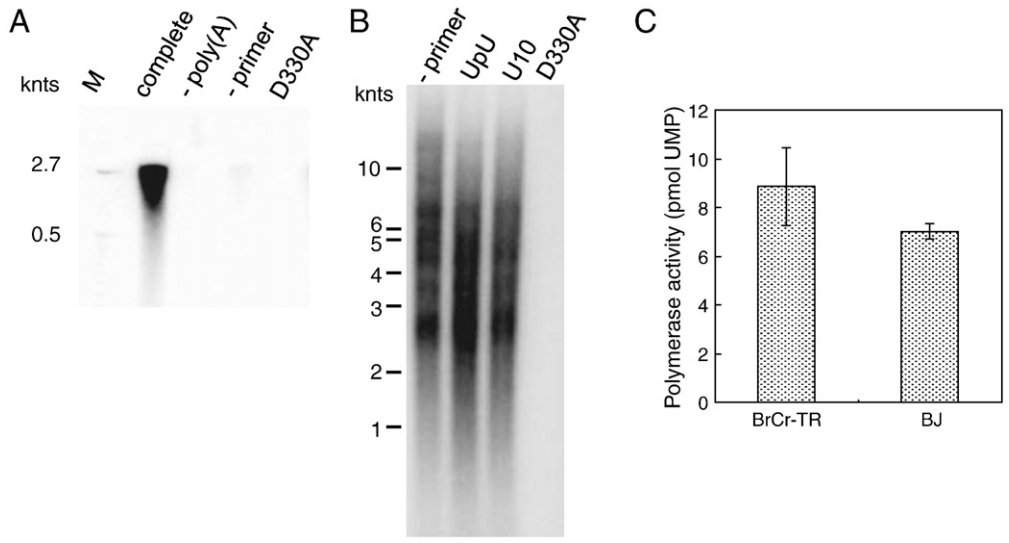

Fig. 3. *In vitro* transcription by EV71 3D^{pol}. A: Representative autoradiograph of EV71 3D^{pol} *in vitro* transcription of poly(A) templates. One hundred nanomolars of EV71 BrCr-TR 3D^{pol} were used in a transcription reaction with 2 mg/ml poly(A) RNA template and 0.5 mM dinucleotide primer UpU under standard transcription conditions (complete). The transcripts were applied to 4% PAGE containing 8 M urea–poly(A): without template–UpU: without primer. D330A: polymerase knockout mutant polymerase. M: [^{32}P]25 bp marker (Promega). The position of the 25 bp marker is indicated on the left. B: *In vitro* transcription of EV71 BrCr-TR genome. EV71 BrCr-TR genome RNA (2 μg/ml) was transcribed by 100 nM of EV71 3D^{pol} in 50 mM Tris–HCl (pH 7.5), 7 mM $MnCl_2$, 100 mM potassium-monoglutamate, 1 mM DTT, 25 μg/ml actinomycin D, 0.05 mM [α-^{32}P] UTP, 200 U/ml RNase inhibitor with or without (-primer) 0.5 μM UpU or U10. RNA products were analyzed by 1.5% agarose gel containing formalin, followed by image analysis by Typhoon Trio plus. The position of the RL10,000 RNA marker is indicated on the left. D330A: polymerase-knockout mutant polymerase. C: Polymerase activity of the EV71 BrCr-TR strain (BrCr-TR) and Beijing isolate (BJ) 3D^{pol}. The mean and standard deviation (error bar) of the polymerase activities were calculated from autoradiograms of three independent experiments.

(Fig. 4E). Polymerase activity was observed at neutral pH (10.5 ± 0.14 pmol UMP at pH 7 and 10.8 ± 0.012 pmol UMP at pH 8), and the highest polymerase activity (12.8 ± 0.42 pmol UMP) was observed at pH 7.5. The polymerase activity decreased at pH 6 and pH 8.5. No activity was observed below pH 5.0 or above pH 8.0.

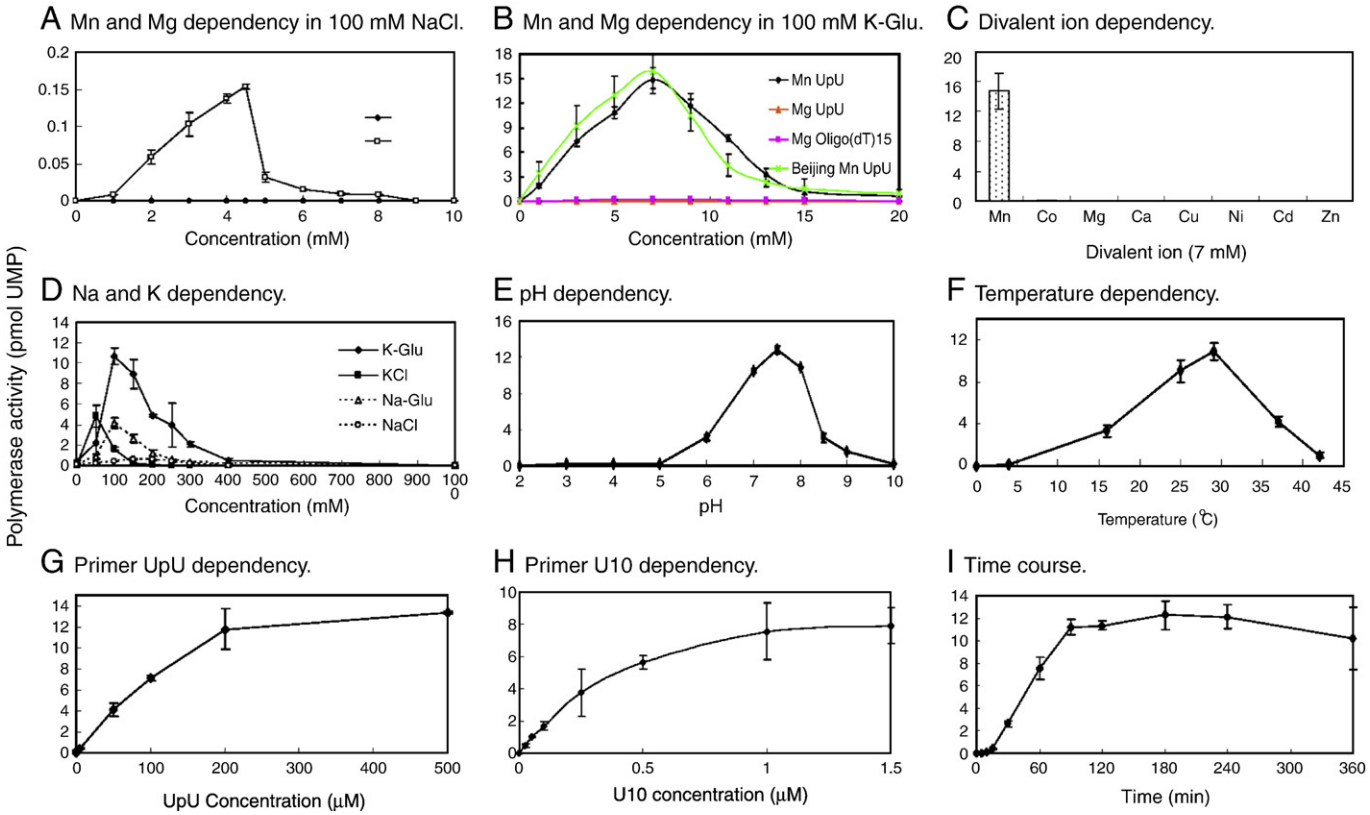

Fig. 4. Biochemical characterization of EV71 3D^{pol}. A: The $MnCl_2$ and $MgCl_2$ dependency of the polymerase activity of EV71 BrCr-TR 3D^{pol} in 100 mM NaCl, B: $MnCl_2$ and $MgCl_2$ dependency of BrCr-TR and BJ 3D^{pol} in 100 mM monopotassium glutamate (UpU and oligo(dT)15 were used as primers); C: divalent cation dependency; D: NaCl, KCl, monosodium glutamate, and monopotassium glutamate dependency in 7 mM $MnCl_2$; E: pH effect; F: temperature effect; G: dinucleotide UpU primer concentration dependency; H: U10 primer concentration dependency, and I: time course (see text). The symbols are indicated in each panel. The mean polymerase activity (incorporated NMP pmol/pmol 3D^{pol}) and standard deviation were calculated from autoradiograms of three independent experiments.

Incubation temperatures were tested at 0, 4, 16, 25, 29, 37, and 42 °C in 50 mM Tris–HCl, pH 7.5, 100 mM potassium-monoglutamate and 7 mM $MnCl_2$ (Fig. 4F). High polymerase activity was obtained between 25 (9.08 ± 1.0 pmol UMP) and 29 °C (10.9 ± 0.75 pmol UMP) with the highest activity seen at 29 °C.

Primer dependency was tested using UpU (Fig. 4G) and the 10 nt U (U10) primers (Fig. 4H). Only trace amounts of UMP incorporation were detected without primers (Fig. 3A). Polymerase activity increased according with the concentration of primers, and plateaued at 200 μM UpU and 1 μM U10.

Finally, polymerase activity was tested at 29 °C for 5, 10, 15, and 30 min, 1, 1.5, 2, 3, 4, and 6 hr (Fig. 4I). The log phase of UMP-incorporation extended from 15 min (0.395 ± 0.022 pmol UMP) to 90 min (11.2 ± 0.70 pmol UMP) and then plateaued. Transcripts were stable up to 6 hr.

3.3. Templates and primers of EV71 $3D^{pol}$

Because the 10 nt U primer showed more effective initiation than UpU (Fig. 4G, H), the priming effects of dinucleotide (ApA, GpG, UpU and CpC), 10 nt (A10, G10, U10 and C10), A32, U16, G18, C27, dT10 and dT15 were each compared at 0.5 μM using homopolymeric templates; poly(U), (C), (A), and (I) (Fig. 5). Poly(I) was used because poly(G) did not have template activity (Fig. S2) [30]. Poly(C) showed strong template activity with and without primers (10.4–13.4 pmol GMP). Poly(U) also showed transcription activity without primers, but the activity was low (0.4 ± 0.09 pmol AMP). Poly(A) or poly(I) did not show transcription activity without primers. For poly(A) and (I) templates, priming activity of 10 nt primers was the highest at 6.5 ± 0.48 pmol UMP and 1.36 ± 0.32 pmol CMP, respectively. That of 10 nt primer for poly(C) was 10.4 ± 1.1 pmol GMP. The priming effect of oligo DNA was also tested because poliovirus $3D^{pol}$ was primed with oligo dT [31]. Oligo dT15 showed stronger priming activity (25.3 ± 1.64 pmol UMP) than U10. The amount of transcription increased according to the length of oligo A primers; 0.39 ± 0.09 (without primer), 0.87 ± 0.15 (ApA), 1.3 ± 0.39 (A10) and 1.6 ± 0.42 pmol AMP (A32), respectively. The effect of primer length was statistically significant (Student's *t* test: $P<0.05$, Fig. 5A).

Transcription of EV71 genome RNA was tested with or without UpU or U10 primers (Fig. 3B). There were no differences in product size and quantity with or without primers. Except for small amounts of the full-length 7 knt product, 2, 3, 4, 5 and 6 knt products were also observed. No transcription was observed when D330A was used.

3.4. RNA binding activity of EV71 $3D^{pol}$

RNA binding of EV71 $3D^{pol}$ was not detected either by the filter binding method (Fig. 6A, S4) or UV-crosslinking experiments (Figs. 6B and C). In the same condition HCV RdRp and influenza virus RdRp bound with RNA. Then, we tried to analyze polymerase RNA binding activity by SPR biosensor analysis with BIAcore (Fig. S5). We used PBS for the analysis because we did not observe RNA binding of EV71 $3D^{pol}$ in the standard transcription buffer. In PBS, poly(G) had the highest affinity for both EV71 and HCV RdRps. However, the response units of the other four RNAs for EV71 $3D^{pol}$ were very low.

3.5. Km and Vmax of EV71 $3D^{pol}$

The kinetic constants (*K*m and *V*max) of EV71 BrCr-TR $3D^{pol}$ were measured using homopolymeric templates (2 mg/ml), 10 nt primers (0.5 μM), and different concentrations of ATP, CTP, GTP and UTP (50, 25, 12.5, 10, 5, 2.5, 2, 1.5, 1, 0.5, 0.25, 0.2, and 0.1 μM) in the optimal transcription buffer. Lineweaver–Burk plots of each incorporated substrate were plotted from each measurement (Fig. 7). *K*m and *V*max were calculated from each plot, and the mean and standard deviation from three independent plots are indicated in Table 1.

3.6. Comparison of the polymerase activity of EV71 clinical isolate

Finally, the polymerase activity of EV71 BJ was examined (Fig. 3C). The polymerase activities of BrCr-TR and BJ were 8.85 ± 1.6 pmol and 7.02 ± 0.31 pmol UMP, respectively. The polymerase activity of the both RdRps with the different concentrations of $MnCl_2$ was compared (Fig. 4B). The $MnCl_2$ dependency curve of both RdRps was similar. *K*m and *V*max for UTP of BJ RdRp were also similar to those of BrCr-TR

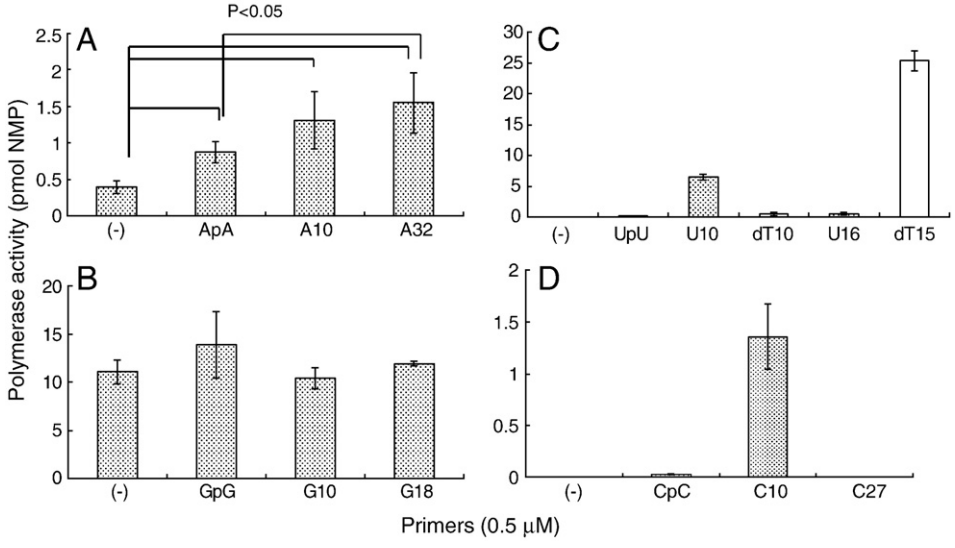

Fig. 5. Primer dependency of EV71 $3D^{pol}$. One hundred nanomolars of EV71 $3D^{pol}$ were incubated at 29 °C for 90 min in 50 mM Tris–HCl (pH 7.5), 100 mM potassium-monoglutamate, 7 mM $MnCl_2$, 1 mM DTT, 25 μg/ml actinomycin D, 200 U/ml human placental RNase inhibitor and 50 μM [α-^{32}P]ATP, 2 mg/ml poly(U) RNA template with or without 0.5 μM of ApA, A10 and A32 primers (A); 50 μM [α-^{32}P]GTP, 2 mg/ml poly(C) RNA template with or without 0.5 μM GpG, G10 and A18 primers (B); 50 μM [α-^{32}P]ATP, 2 mg/ml poly(A) RNA template with or without 0.5 μM of UpU, U10, U16, dT10 and dT15 primers (C); and 50 μM [α-^{32}P]CTP, 2 mg/ml poly(I) RNA template with or without 0.5 μM of CpC, C10 and C27 primers (D). The mean polymerase activity (incorporated NMP pmol/pmol $3D^{pol}$) and standard deviation were calculated from autoradiograms of three independent experiments.

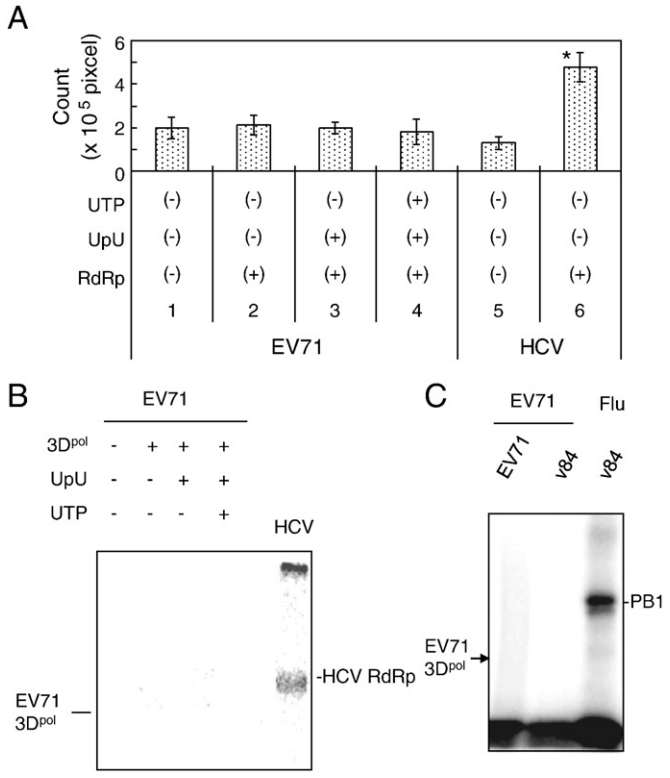

Fig. 6. RNA binding assay of EV71 3D^{pol}. A. The filter binding assay of EV71 3D^{pol} with or without 0.5 mM UpU or 0.5 mM UTP and [^{32}P]-EV71 BrCr-TR genome RNA (EV71). HCV JFH1 NS5B RdRp was used as a positive control. The mean and standard error (error bar) of the pixcel numbers were calculated from three independent measurements (Fig. S4). *$p<0.001$ (Student's *t* test). B. UV-crosslink assay of EV71 3D^{pol} with or without 0.5 mM UpU or 0.5 mM UTP and [^{32}P]-EV71 BrCr-TR genome RNA (EV71). HCV RdRp was used as a positive control (HCV). The positions of EV71 3D^{pol} (53.1 kDa) and HCV RdRp (65.3 kDa) are indicated. C. UV-crosslink assay of EV71 3D^{pol} with [^{32}P]-EV71 BrCr-TR genome RNA (EV71) and [^{32}P]-influenza virus v84 model RNA template (v84). Influenza virus RdRp was used as a positive control (Flu). The positions of EV71 3D^{pol} (53.1 kDa) and influenza virus RdRp PB1 subunit (86.6 kDa) are indicated.

(Table 1, Fig. 7). These data indicate that the RdRps from two different strains have similar activities.

4. Discussion

In the last decade EV71 infection has significantly increased in the Western Pacific Region [23], and particularly in China unusual EV71 epidemic has started since 2008 [17–19]. In order to understand their replication mechanisms and to develop a control strategy against EV71 infection, we analyzed the biochemical characteristics of 3D^{pol} of BrCr-TR and the Chinese isolate (BJ) isolated from a severely ill patient in Beijing, 2008.

All polymerases adopt a similar canonical folded structure resembling a cupped right hand with finger, palm, and thumb subdomains. The most conserved structural element of the RdRp subdomain is the catalytic palm subdomain, in which two catalytic aspartic acid side chains coordinately bind to two divalent metal ions that are essential for catalysis [32]. The finger and thumb subdomains are involved in template, primer, and NTP substrate binding. The conformation of the thumb subdomain is related to the mode of initiation of the RdRp, i.e., whether initiation is primer dependent or primer independent (*de novo*) [33]. When the GDD (residues 329–331) sequence in motif C was mutated to GAD, EV71 3D^{pol}D330A lost polymerase activity (Figs. 3A and B), confirming that this sequence is the polymerase active site (Fig. S7).

All DNA and RNA polymerases require two divalent cations to catalyze phosphoryl transfer, and Mg^{2+} is the most commonly employed cation [34]. Enterovirus 3D^{pol} such as poliovirus, rhinovirus, FMDV, and CVA show activity with both Mg^{2+} and Mn^{2+} [35–37], and their crystal structures are similar [38]. However, our EV71 3D^{pol} is an Mn^{2+}-specific polymerase, and none of the other divalent cations analyzed so far, including Mg^{2+}, has shown any polymerase activity, although weak activity was observed with Co^{2+} (Figs. 4A–C). Chen et al. detected polymerase activity with EV71 3D^{pol} purified from bacteria at 5 mM $MgCl_2$ [21], which is controversial to our finding. The processing of the N-terminus of 3D^{pol} by the ubiquitin-specific carboxy-terminal protease may change the conformation of 3D^{pol} to affect the divalent cation dependence of the polymerase. Ni^{2+} coordinates with 271H, 273H and 282C of EV71 3D^{pol} [22]. However, it may not affect the RdRp activity because no RdRp activity was detected with Ni^{2+} (Fig. 4C).

Mn^{2+} cations relax the nucleotide specificity of polymerases [39,40] as well as their template specificity [41]. Glutamate ions alter the sensitivity of the enzyme to $MnCl_2$ (Figs. 4A and B). The Mg^{2+} concentration in cells varies between 14 and 20 mM, and the cation is distributed almost equally in the nuclear, mitochondrial, and the cytosolic and endoplasmic reticulum cellular compartments [42]. The Mn^{2+} concentration in cells varies from report to report [43,44]. Although Mn^{2+} also permits polymerases to incorporate incorrect sugar configurations [39,45], EV71 3D^{pol} did not show reverse transcriptase activity with a poly(A) template together with oligo dT primers (Fig. S3). Mn^{2+} also relaxes the template specificity of polymerases [41], and we found that the cation contributed to EV71 genome recombination, together with the low RNA binding activity of EV71 3D^{pol} (Fig. 6, S4) [46–49]. RNA binding activity of poliovirus and FMDV 3D^{pol} is stronger than that of EV71 3D^{pol} because poliovirus and FMDV 3D^{pol} can be detected by the filter binding method [50,51]. EV71 3D^{pol} functioned at neutral pH and low salt concentrations (Fig. 4), as seen with other picornavirus 3D^{pol} [2,37,50]. Terminal nucleotidyl transferase activity was not observed with our purified EV71 3D^{pol} (Fig. S6) although HRV 3D^{pol} incorporates TTP [36]. The explanation for the lack of EV71 3D^{pol} activity with Mg^{2+} is not clear because the RdRp motif primary sequence of 3D^{pol} from EV71, HRV, CVA to poliovirus are similar (Fig. S7) and because the divalent ions were not indicated in its crystallography [22]. Only EV71 3D^{pol} has unique 226P and 228S residues in motif A, which is proximal to the divalent ion interacting residue, 238D (Fig. S7) [32]. However, P226D and P226D/S228H mutants did not show polymerase activity with Mg^{2+} either (data not shown).

Picornavirus 3D^{pol} are primer-dependent and initiate viral transcription and replication with VPg [33], but purified poliovirus and HRV-16 3D^{pol} transcribed in both primer-dependent and independent manners [31,36]. For EV71 3D^{pol}, polymerase activity of poly(A) and poly(C) was at least five times greater than the other homopolymeric templates (Fig. 5). EV71 3D^{pol} requires primers for poly(A), poly(U) and poly(I) templates, but does not require primers for the poly(C) template as does poliovirus 3D^{pol} [31]. Although picornavirus 3D^{pol} utilize protein primers in infected cells, the ability of these enzymes to biochemically catalyze *de novo* RNA synthesis with poly(C) may have significant implications for viral genome replication. HRV-16 3D^{pol} does not use poly(G) or poly(U) templates [36]. The stability of the primer-template duplex may enhance transcription initiation, and high concentrations of dinucleotide also promoted efficient transcription initiation. The melting temperatures (Tm) of U10, U16, dT15 and dT10 are 53.5 °C, 61.4 °C, 18.3 °C and 12.2 °C, respectively (MELTING 4.2) [52], and dT15 showed the highest transcription activity for poly (A) at 29 °C (Fig. 5C). Under the optimal *in vitro* transcription conditions, EV71 3D^{pol} transcribed EV71 genome RNA with several subgenomic-sized products (Fig. 3B). The effect of primers on genome-size transcription was not observed, indicating *de novo* initiation or hairpin initiation.

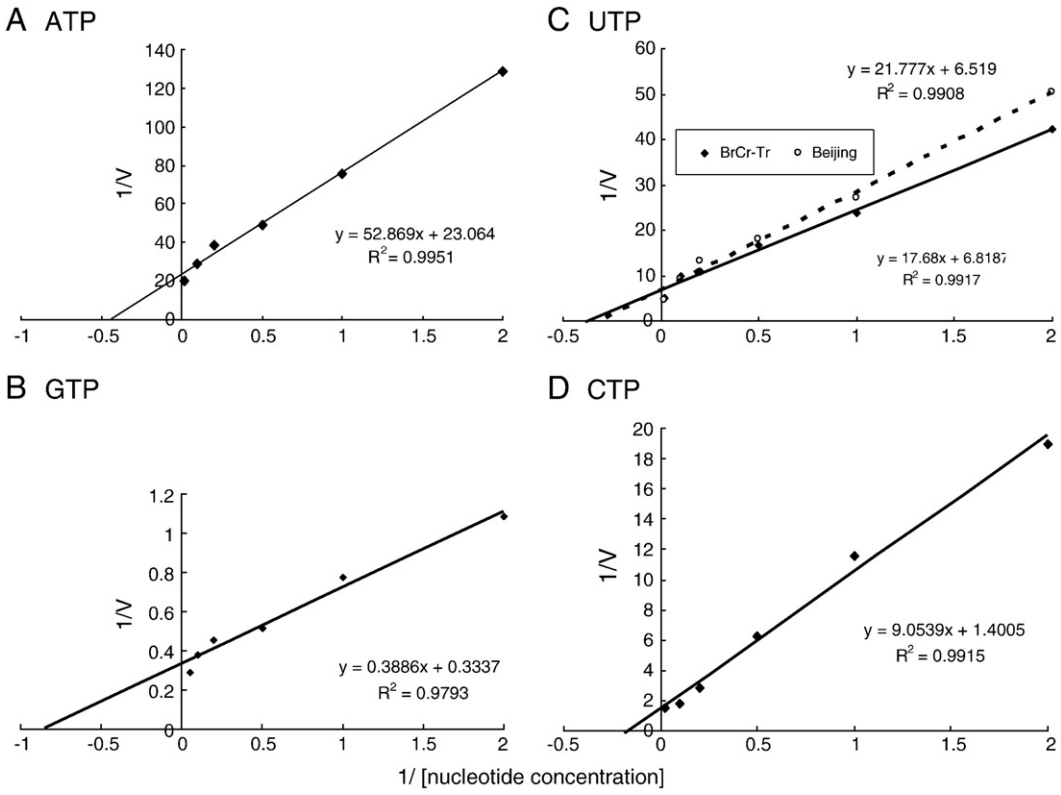

Fig. 7. Lineweaver–Burk plots of EV71 3D^{pol}. For kinetic analysis, 100 nM of EV 71 BrCr-TR 3D^{pol} was incubated for 1 hr using homopolymeric templates (2 mg/ml), 10-nucleotide primers (0.5 μM), and different concentrations of [α-^{32}P]ATP, [α-^{32}P]GTP, [α-^{32}P]UTP and [α-^{32}P]CTP. That of Beijing 3D^{pol} was also indicated (broken line). Lineweaver–Burk plots were derived from three independent experiments.

Table 1
Km and *Vmax* of EV71 3D polymerase.

	ATP	CTP	GTP	UTP
Km (μM)	2.35 ± 0.05	5.40 ± 0.93	1.12 ± 0.10	2.81 ± 0.31
Km of BJ (μM)	nd*	nd	nd	3.46 ± 0.37
Vmax (/min)	0.00078 ± 0.00005	0.011 ± 0.0017	0.050 ± 0.0043	0.0027 ± 0.0005
Vmax of BJ (/min)	nd	nd	nd	0.0025 ± 0.0003

* Not done.

EV71 3D^{pol} did not show terminal nucleotidyl transferase activity because random elongation from primers nor templates were not observed (Fig. S2, S6) although in another study poliovirus 3D^{pol} showed this activity [53]. EV71 3D^{pol} formed monomers under the transcription conditions of this study (Fig. 3) although poliovirus 3D^{pol} formed oligomers [51,54,55].

The kinetic constants (*Km* and *Vmax*) of EV71 3D^{pol} were calculated from classical Lineweaver–Burk plots (Fig. 7, Table 1). The *Km* value for the EV71 3D^{pol} is smaller than the *Km* values for both the influenza A virus RdRp [56] and poliovirus 3D^{pol} [57], but similar to the *Km* value for the RdRps from both HCV JFH1 [27] and HRV-16 [36]. The *Vmax* values for the EV71 3D^{pol} are similar to those of FMDV and HRV-16 3D^{pol} [36,50], and much smaller than those of poliovirus 3D^{pol} (4.4/min for UTP and 16.8/min for GTP in primer-dependent transcription and 3.4/min for GTP in *de novo* transcription) [31]. The small *Km* for GTP agreed with the finding of crystallography [22]. The large *Vmax* of EV71 3D^{pol} for GTP indicates the potential for treatment of EV71 infection with the antiviral drug ribavirin although it is not efficient because of the small *Km* for GTP [58]. According to its *Km* and *Vmax* CTP analogues can be tested for EV71 inhibition.

The weak RNA template binding of EV71 3D^{pol} may affect the *Vmax* obtained with our *in vitro* transcription system. The viral protein 3AB has been shown to enhance the RNA binding of poliovirus 3D^{pol} and leads to enhanced transcription [59]. Other EV71 proteins may affect the RNA template binding affinity of 3D^{pol}, and the RNA polymerization rate of the EV71 replication complex in infected cells may be faster than these values that we acquired *in vitro*.

The 3D^{pol} of the different genotype, which was isolated from the severely ill patient, showed similar polymerase activity (Table 1, Figs. 3C and 4B), indicating that 3D^{pol} is a good target for the control of EV71 infection, but not a determinant of the pathogenicity of the recent Chinese epidemic strains.

Supplementary materials related to this article can be found online at doi:10.1016/j.bbagrm.2011.01.001.

Acknowledgements

This work was supported by Grants-in-aid from the Chinese Academy of Sciences (0514P51131) and the Li Kashing Foundation (0682P11131).

References

[1] M. Pallansch, R. Roos, Fields Virology, 5th ed.Lippincott Williams & Wilkins, New York, 2007.
[2] A.V. Paul, E. Rieder, D.W. Kim, J.H. van Boom, E. Wimmer, Identification of an RNA hairpin in poliovirus RNA that serves as the primary template in the in vitro uridylylation of VPg, J. Virol. 74 (2000) 10359–10370.
[3] B.A. Brown, M.S. Oberste, J.P. Alexander Jr., M.L. Kennett, M.A. Pallansch, Molecular epidemiology and evolution of enterovirus 71 strains isolated from 1970 to 1998, J. Virol. 73 (1999) 9969–9975.
[4] M.J. Cardosa, D. Perera, B.A. Brown, D. Cheon, H.M. Chan, K.P. Chan, H. Cho, P. McMinn, Molecular epidemiology of human enterovirus 71 strains and recent outbreaks in the Asia-Pacific region: comparative analysis of the VP1 and VP4 genes, Emerg. Infect. Dis. 9 (2003) 461–468.
[5] P. McMinn, K. Lindsay, D. Perera, H.M. Chan, K.P. Chan, M.J. Cardosa, Phylogenetic analysis of enterovirus 71 strains isolated during linked epidemics in Malaysia, Singapore, and Western Australia, J. Virol. 75 (2001) 7732–7738.
[6] P.V. Tu, N.T. Thao, D. Perera, T.K. Huu, N.T. Tien, T.C. Thuong, O.M. How, M.J. Cardosa, P.C. McMinn, Epidemiologic and virologic investigation of hand, foot, and mouth disease, southern Vietnam, 2005, Emerg. Infect. Dis. 13 (2007) 1733–1741.
[7] K. Mizuta, C. Abiko, T. Murata, Y. Matsuzaki, T. Itagaki, K. Sanjoh, M. Sakamoto, S. Hongo, S. Murayama, K. Hayasaka, Frequent importation of enterovirus 71 from surrounding countries into the local community of Yamagata, Japan, between 1998 and 2003, J. Clin. Microbiol. 43 (2005) 6171–6175.
[8] P.C. McMinn, An overview of the evolution of enterovirus 71 and its clinical and public health significance, FEMS Microbiol. Rev. 26 (2002) 91–107.
[9] S. Abubakar, H.Y. Chee, N. Shafee, K.B. Chua, S.K. Lam, Molecular detection of enteroviruses from an outbreak of hand, foot and mouth disease in Malaysia in 1997, Scand. J. Infect. Dis. 31 (1999) 331–335.
[10] M. Ho, E.R. Chen, K.H. Hsu, S.J. Twu, K.T. Chen, S.F. Tsai, J.R. Wang, S.R. Shih, An epidemic of enterovirus 71 infection in Taiwan. Taiwan Enterovirus Epidemic Working Group, N. Engl. J. Med. 341 (1999) 929–935.
[11] C.Y. Lu, C.Y. Lee, C.L. Kao, W.Y. Shao, P.I. Lee, S.J. Twu, C.C. Yeh, S.C. Lin, W.Y. Shih, S.I. Wu, L.M. Huang, Incidence and case-fatality rates resulting from the 1998 enterovirus 71 outbreak in Taiwan, J. Med. Virol. 67 (2002) 217–223.
[12] L.Y. Chang, Enterovirus 71 in Taiwan, Pediatr. neonatol. 49 (2008) 103–112.
[13] C.C. Huang, C.C. Liu, Y.C. Chang, C.Y. Chen, S.T. Wang, T.F. Yeh, Neurologic complications in children with enterovirus 71 infection, N. Engl. J. Med. 341 (1999) 936–942.
[14] H. Komatsu, Y. Shimizu, Y. Takeuchi, H. Ishiko, H. Takada, Outbreak of severe neurologic involvement associated with enterovirus 71 infection, Pediatr. Neurol. 20 (1999) 17–23.
[15] L.C. Lum, K.T. Wong, S.K. Lam, K.B. Chua, A.Y. Goh, W.L. Lim, B.B. Ong, G. Paul, S. AbuBakar, M. Lambert, Fatal enterovirus 71 encephalomyelitis, J. Pediatr. 133 (1998) 795–798.
[16] S.M. Wang, C.C. Liu, H.W. Tseng, J.R. Wang, C.C. Huang, Y.J. Chen, Y.J. Yang, S.J. Lin, T.F. Yeh, Clinical spectrum of enterovirus 71 infection in children in southern Taiwan, with an emphasis on neurological complications, Clin. Infect. Dis. 29 (1999) 184–190.
[17] H. Song, S. Shih, Y. L., H. Zhuang, Advances in the study of enterovirus 71 infection, J. Pathogen Biol. 3 (2008) 947–949.
[18] F. Yang, L. Ren, Z. Xiong, J. Li, Y. Xiao, R. Zhao, Y. He, G. Bu, S. Zhou, J. Wang, J. Qi, Enterovirus 71 outbreak in the People's Republic of China in 2008, J. Clin. Microbiol. 47 (2009) 2351–2352.
[19] Y. Zhang, X.J. Tan, H.Y. Wang, D.M. Yan, S.L. Zhu, D.Y. Wang, F. Ji, X.J. Wang, Y.J. Gao, L. Chen, H.Q. An, D.X. Li, S.W. Wang, A.Q. Xu, Z.J. Wang, W.B. Xu, An outbreak of hand, foot, and mouth disease associated with subgenotype C4 of human enterovirus 71 in Shandong, China, J. Clin. Virol. 44 (2009) 262–267.
[20] J.H. Chern, K.S. Shia, T.A. Hsu, C.L. Tai, C.C. Lee, Y.C. Lee, C.S. Chang, S.N. Tseng, S.R. Shih, Design, synthesis, and structure-activity relationships of pyrazolo[3, 4-d] pyrimidines: a novel class of potent enterovirus inhibitors, Bioorg. Med. Chem. Lett. 14 (2004) 2519–2525.
[21] T.C. Chen, H.Y. Chang, P.F. Lin, J.H. Chern, J.T. Hsu, C.Y. Chang, S.R. Shih, Novel antiviral agent DTriP-22 targets RNA-dependent RNA polymerase of enterovirus 71, Antimicrob. Agents Chemother. 53 (2009) 2740–2747.
[22] Y. Wu, L. Z., Y. Miao, Y. Yu, D. H., P. Wei, M. Bartlam, L. X., R. Z., Structures of EV71 RNA-dependent RNA polymerase in complex with substrate and analogue provide a drug target against the hand-foot-and-mouth disease pandemic in China, Protein, Cell 1 (2010) 491–500.
[23] J.M. Bible, P. Pantelidis, P.K. Chan, C.Y. Tong, Genetic evolution of enterovirus 71: epidemiological and pathological implications, Rev. Med. Virol. 17 (2007) 371–379.
[24] M. Arita, H. Shimizu, N. Nagata, Y. Ami, Y. Suzaki, T. Sata, T. Iwasaki, T. Miyamura, Temperature-sensitive mutants of enterovirus 71 show attenuation in cynomolgus monkeys, J. Gen. Virol. 86 (2005) 1391–1401.
[25] A. Murayama, L. Weng, T. Date, D. Akazawa, X. Tian, T. Suzuki, T. Kato, Y. Tanaka, M. Mizokami, T. Wakita, T. Toyoda, RNA polymerase activity and specific RNA structure are required for efficient HCV replication in cultured cells, PLoS Pathog. 6 (2010) e1000885.
[26] J.J. Arnold, C.E. Cameron, Poliovirus RNA-dependent RNA polymerase (3D(pol)). Assembly of stable, elongation-competent complexes by using a symmetrical primer-template substrate (sym/sub), J. Biol. Chem. 275 (2000) 5329–5336.
[27] L. Weng, J. Du, J. Zhou, J. Ding, T. Wakita, M. Kohara, T. Toyoda, Modification of hepatitis C virus 1b RNA polymerase to make high-active JFH1 type polymerase by mutation of thumb domain, Arch. Virol. 154 (2009) 765–773.
[28] M.S. Oberste, J.B. Flanegan, Measurement of poliovirus RNA polymerase binding to poliovirion and nonviral RNAs using a filter-binding assay, Nucleic Acids Res. 16 (1988) 10339–10352.
[29] M. Kobayashi, T. Toyoda, A. Ishihama, Influenza virus PB1 protein is the minimal and essential subunit of RNA polymerase, Arch. Virol. 141 (1996) 525–539.
[30] G. Luo, R.K. Hamatake, D.M. Mathis, J. Racela, K.L. Rigat, J. Lemm, R.J. Colonno, De novo initiation of RNA synthesis by the RNA-dependent RNA polymerase (NS5B) of hepatitis C virus, J. Virol. 74 (2000) 851–863.
[31] J.J. Arnold, C.E. Cameron, Poliovirus RNA-dependent RNA polymerase (3Dpol) is sufficient for template switching in vitro, J. Biol. Chem. 274 (1999) 2706–2716.
[32] T.A. Steitz, DNA polymerases: structural diversity and common mechanisms, J. Biol. Chem. 274 (1999) 17395–17398.
[33] C. Ferrer-Orta, A. Arias, C. Escarmis, N. Verdaguer, A comparison of viral RNA-dependent RNA polymerases, Curr. Opin. Struct. Biol. 16 (2006) 27–34.
[34] C.A. Brautigam, T.A. Steitz, Structural and functional insights provided by crystal structures of DNA polymerases and their substrate complexes, Curr. Opin. Struct. Biol. 8 (1998) 54–63.
[35] A. Arias, J.J. Arnold, M. Sierra, E.D. Smidansky, E. Domingo, C.E. Cameron, Determinants of RNA-dependent RNA polymerase (in)fidelity revealed by kinetic analysis of the polymerase encoded by a foot-and-mouth disease virus mutant with reduced sensitivity to ribavirin, J. Virol. 82 (2008) 12346–12355.
[36] M. Hung, C.S. Gibbs, M. Tsiang, Biochemical characterization of rhinovirus RNA-dependent RNA polymerase, Antivir. Res. 56 (2002) 99–114.
[37] A. Gruez, B. Selisko, M. Roberts, G. Bricogne, C. Bussetta, I. Jabafi, B. Coutard, A.M. De Palma, J. Neyts, B. Canard, The crystal structure of coxsackievirus B3 RNA-dependent RNA polymerase in complex with its protein primer VPg confirms the existence of a second VPg binding site on Picornaviridae polymerases, J. Virol. 82 (2008) 9577–9590.
[38] G. Campagnola, M. Weygandt, K. Scoggin, O. Peersen, Crystal structure of coxsackievirus B3 3Dpol highlights the functional importance of residue 5 in picornavirus polymerases, J. Virol. 82 (2008) 9458–9464.
[39] S. Tabor, C.C. Richardson, Effect of manganese ions on the incorporation of dideoxynucleotides by bacteriophage T7 DNA polymerase and Escherichia coli DNA polymerase I, Proc. Natl. Acad. Sci. U. S. A. 86 (1989) 4076–4080.
[40] Y. Huang, A. Beaudry, J. McSwiggen, R. Sousa, Determinants of ribose specificity in RNA polymerization: effects of Mn2+ and deoxynucleoside monophosphate incorporation into transcripts, Biochemistry 36 (1997) 13718–13728.
[41] A. Palmenberg, P. Kaesberg, Synthesis of complementary strands of heterologous RNAs with Qbeta replicase, Proc. Natl. Acad. Sci. U. S. A. 71 (1974) 1371–1375.
[42] A. Romani, Regulation of magnesium homeostasis and transport in mammalian cells, Arch. Biochem. Biophys. 458 (2007) 90–102.
[43] M. Morello, A. Canini, P. Mattioli, R.P. Sorge, A. Alimonti, B. Bocca, G. Forte, A. Martorana, G. Bernardi, G. Sancesario, Sub-cellular localization of manganese in the basal ganglia of normal and manganese-treated rats. An electron spectroscopy imaging and electron energy-loss spectroscopy study, Neurotoxicology 29 (2008) 60–72.
[44] K. Kalia, W. Jiang, W. Zheng, Manganese accumulates primarily in nuclei of cultured brain cells, Neurotoxicology 29 (2008) 466–470.
[45] D.W. Gohara, S. Crotty, J.J. Arnold, J.D. Yoder, R. Andino, C.E. Cameron, Poliovirus RNA-dependent RNA polymerase (3Dpol): structural, biochemical, and biological analysis of conserved structural motifs A and B, J. Biol. Chem. 275 (2000) 25523–25532.
[46] X. Chen, Q. Zhang, J. Li, W. Cao, J.X. Zhang, L. Zhang, W. Zhang, Z.J. Shao, Y. Yan, Analysis of recombination and natural selection in human enterovirus 71, Virology 398 (2010) 251–261.
[47] N.Z. Ding, X.M. Wang, S.W. Sun, Q. Song, S.N. Li, C.Q. He, Appearance of mosaic enterovirus 71 in the 2008 outbreak of China, Virus Res. (2009).
[48] S.C. Huang, Y.W. Hsu, H.C. Wang, S.W. Huang, D. Kiang, H.P. Tsai, S.M. Wang, C.C. Liu, K.H. Lin, I.J. Su, J.R. Wang, Appearance of intratypic recombination of enterovirus 71 in Taiwan from 2002 to 2005, Virus Res. 131 (2008) 250–259.
[49] Y. Zhang, Z. Zhu, W. Yang, J. Ren, X. Tan, Y. Wang, N. Mao, S. Xu, S. Zhu, A. Cui, Y. Zhang, D. Yan, Q. Li, X. Dong, J. Zhang, Y. Zhao, J. Wan, Z. Feng, J. Sun, S. Wang, D. Li, W. Xu, An emerging recombinant human enterovirus 71 responsible for the 2008 outbreak of Hand Foot and Mouth Disease in Fuyang city of China, Virol. J. 7 (2010) 94.
[50] A. Arias, R. Agudo, C. Ferrer-Orta, R. Perez-Luque, A. Airaksinen, E. Brocchi, E. Domingo, N. Verdaguer, C. Escarmis, Mutant viral polymerase in the transition of virus to error catastrophe identifies a critical site for RNA binding, J. Mol. Biol. 353 (2005) 1021–1032.
[51] J.D. Pata, S.C. Schultz, K. Kirkegaard, Functional oligomerization of poliovirus RNA-dependent RNA polymerase, RNA (New York, N.Y.) 1 (1995) 466–477.
[52] N. Le Novere, MELTING, computing the melting temperature of nucleic acid duplex, Bioinformatics (Oxford, England) 17 (2001) 1226–1227.
[53] K.L. Neufeld, J.M. Galarza, O.C. Richards, D.F. Summers, E. Ehrenfeld, Identification of terminal adenylyl transferase activity of the poliovirus polymerase 3Dpol, J. Virol. 68 (1994) 5811–5818.
[54] J.L. Hansen, A.M. Long, S.C. Schultz, Structure of the RNA-dependent RNA polymerase of poliovirus, Structure 5 (1997) 1109–1122.
[55] M.T. Beckman, K. Kirkegaard, Site size of cooperative single-stranded RNA binding by poliovirus RNA-dependent RNA polymerase, J. Biol. Chem. 273 (1998) 6724–6730.
[56] S. Zhang, L. Weng, L. Geng, J. Wang, J. Zhou, V. Deubel, P. Buchy, T. Toyoda, Biochemical and kinetic analysis of the influenza virus RNA polymerase purified from insect cells, Biochem. Biophys. Res. Commun. 391 (2010) 570–574.
[57] J.J. Arnold, S.K. Ghosh, C.E. Cameron, Poliovirus RNA-dependent RNA polymerase (3D(pol)). Divalent cation modulation of primer, template, and nucleotide selection, J. Biol. Chem. 274 (1999) 37060–37069.
[58] Z.H. Li, C.M. Li, P. Ling, F.H. Shen, S.H. Chen, C.C. Liu, C.K. Yu, S.H. Chen, Ribavirin reduces mortality in enterovirus 71-infected mice by decreasing viral replication, J. Infect. Dis. 197 (2008) 854–857.
[59] A.V. Paul, X. Cao, K.S. Harris, J. Lama, E. Wimmer, Studies with poliovirus polymerase 3Dpol. Stimulation of poly(U) synthesis in vitro by purified poliovirus protein 3AB, J. Biol. Chem. 269 (1994) 29173–29181.